Title
Proteomic mapping of p53 immunogenicity in pancreatic, ovarian, and breast cancers

Journal
Proteomics Clinical Applications, 10(7)

ISSN
1862-8346

Authors
Katchman, Benjamin A
Barderas, Rodrigo
Alam, Rizwan
et al.

Publication Date
2016-07-01

DOI
10.1002/prca.201500096

Peer reviewed

HHS Public Access

Author manuscript

Proteomics Clin Appl. Author manuscript; available in PMC 2017 August 11.

Published in final edited form as:

Proteomics Clin Appl. 2016 July ; 10(7): 720–731. doi:10.1002/prca.201500096.

Proteomic mapping of p53 immunogenicity in pancreatic, ovarian, and breast cancers

Benjamin A. Katchman[1], **Rodrigo Barderas**[2], **Rizwan Alam**[1], **Diego Chowell**[1], **Matthew S. Field**[1], **Laura J. Esserman**[3], **Garrick Wallstrom**[1], **Joshua LaBaer**[1], **Daniel W. Cramer**[4], **Michael A. Hollingsworth**[5], and **Karen S. Anderson**[1]

[1]Virginia G. Piper Center for Personalized Diagnostics, Biodesign Institute, Arizona State University, Tempe, AZ, USA

[2]Biochemistry and Molecular Biology I Department, Complutense University, Madrid, Spain

[3]Department of Surgery, University of California, San Francisco, CA, USA

[4]Department of Gynecology and Reproductive Biology, Brigham and Women's Hospital, Boston, MA

[5]Eppley Institute for Research in Cancer and Allied Diseases, University of Nebraska Medical Center, Omaha, Nebraska, USA

Abstract

Purpose—Mutations in *TP53* induce autoantibody immune responses in a subset of cancer patients, which have been proposed as biomarkers for early detection. Here, we investigate the association of p53-specific autoantibodies with multiple tumor subtypes and determine the association with p53 mutation status and epitope specificity.

Experimental design—IgG p53 autoantibodies (p53-AAb), were quantified in 412 serum samples using a programmable ELISA assay from patients with serous ovarian, pancreatic adenocarcinoma, and breast cancer. To determine if patients generated mutation-specific autoantibodies we designed a panel of the most relevant 51 p53 point mutant proteins, to be displayed on custom programmable protein microarrays. To determine the epitope specificity we displayed 12 overlapping tiling fragments and 38 N- and C-terminal deletions spanning the length of the wild-type p53 protein.

Results—We detected p53-AAb with sensitivities of 58.8% (ovarian), 22% (pancreatic), 32% (triple negative breast cancer), and 10.2% (HER2+ breast cancer) at 94% specificity. Sera with p53-AAb contained broadly reactive autoantibodies to 51 displayed p53 mutant proteins, demonstrating a polyclonal response to common epitopes. All p53-AAb displayed broad polyclonal immune response to both continuous and discontinuous epitopes at the N- and C-terminus as well as the DNA-binding domain.

Correspondence: Dr. Karen S. Anderson, Biodesign Institute, Arizona State University, PO Box 876401, Tempe, AZ 85287, USA Karen.Anderson.1@asu.edu.

Additional supporting information may be found in the online version of this article at the publisher's web-site

Conclusion and clinical relevance—In this comprehensive analysis, mutations in tumor p53 induce strong, polyclonal autoantibodies with broadly reactive epitope specificity.

Keywords

Antibody mapping; Autoantibody; Cancer; p53; Protein array

1 Introduction

Naturally occurring antibodies are biomarkers of many autoimmune, infectious, and malignant diseases, and are used for both diagnosis and disease monitoring. Humoral immune responses are polyclonal responses, which recognize linear and/or conformational immunogenic epitopes within the same protein [1, 2]. Recent advances in native protein display technologies suggest that conformational-dependent discontinuous epitopes may represent up to 90% of the total B-cell response and are often dependent on the secondary or tertiary structure of proteins [3]. Developing high-throughput methodologies for conformational and linear protein display will be essential to identify the diversity and specificity of immunogenic epitopes.

TP53 is mutated in greater than 50% of all cancers; 95% of these mutations are missense mutations that alter the function and regulation of p53 [4]. Mutations in *TP53* increase the stability of p53 protein, leading to an accumulation and increase in antigen presentation of this highly immunogenic protein [4]. We and others have identified p53-specific autoantibodies (AAb) in the sera of pancreatic adenocarcinoma (PDAC), serous ovarian (SOC), and breast cancer (BC) patients as potential biomarkers for early detection and prognosis [5–8]. Patients with p53-AAb at the time of diagnosis of colorectal cancer have a worse overall survival [7], but in SOC, p53-AAb correlate with increased overall survival [6]. This contradiction likely reflects the confounding impact of p53 mutation itself and the functional significance of these AAb remains unknown [7, 9]. Despite the strong specificity of p53-AAb in the sera of cancer patients, only 5–20% of patients with cancers harboring *TP53* missense mutations will have detectable p53-AAb by traditional ELISA assays, which has limited their use as diagnostic markers and stresses the need for improved diagnostic assays [10].

Patients with p53-mutant tumors frequently develop AAb to the wild-type (WT) p53 protein [11]. Two large-scale studies have used overlapping peptides (15 amino acids each with 10 amino acid overlap) spanning the entire length of WT-p53, for epitope mapping in multiple tumor types [11, 12]. Both studies mapped the dominant immunogenic epitopes to the N- and C-terminal (nonmutated) regions of the molecule. However, subdominant epitopes within the DNA-binding domain were also identified in preclinical serum samples, providing preliminary evidence to support the clinical utility of p53-AAb as a screening tool for colorectal cancer [12]. Structural studies confirm that the N- and C-terminal regions of p53 are highly exposed and accessible at the protein surface, while the central region (DNA-binding domain) is buried in the interior of the molecule [13]. However, conformational and mutation-specific epitopes have not been studied.

Recent advances in protein display technologies now permit rapid, detailed mapping of conformational-specific immunogenic epitopes. Using programmable protein display (NAPPA) and RAPID ELISA tagged proteins are expressed in situ using mammalian lysate and captured by protein tags [6,14]. The overall objective of this study was to determine the correlation of AAb to WT, mutant, linear, and conformational epitopes of p53 with tumor type and mutation status. We first screened a total of 412 serum samples from SOC, PDAC, and BC (TNBC, HER2+, and ER+) for AAb to full-length WT-p53 protein to evaluate the sensitivity and specificity of p53-AAb for cancer detection. We evaluated the correlation between tumor *TP53* mutation status and the presence of epitope specificity of p53-AAb. We developed custom NAPPA arrays expressing 51 of the most common p53 point mutations for detection of antibodies in patient serum [14,15]. We then adapted this technology for epitope mapping by displaying overlapping linear peptides, as well as N- and C-terminal deletions spanning the entire length of p53. This permitted the simultaneous expression of both continuous and discontinuous epitopes. The display of specific epitopes on the array was confirmed using monoclonal antibodies, then used to map p53-AAb epitopes in the sera of cancer patients. This is the first comprehensive study over multiple tumor types to correlate the antibodies against specific p53 epitopes with p53 mutation status and tumor type.

2 Materials and methods

2.1 Patient sera

Sera from patients with pancreatic cancer were obtained from The University of Nebraska Medical Center pancreatic biorepository. Sera were obtained from patients with stage III or IV pancreatic cancer following rapid autopsy within 2–3 h of death. Control sera were derived from patients with high CA19-9 serum levels and benign pancreatic diseases (clinical characteristics are currently unavailable). We utilized a total of 60 cases and 63 benign disease controls, subsets of this sample set were used for various assays.

Sera from patients with serous ovarian cancer were obtained from the Brigham and Women's Hospital. Sera derived from ovarian cancer patients were obtained at the time of presentation prior to surgery. Sera from age, gender, and location matched general population control women were obtained using a standardized serum collection protocol and stored at −80°C until use. Cases and matched controls were processed simultaneously. Women with a personal history of cancer (other than nonmelanoma skin cancer) were excluded as controls (Case $n = 17$, Control $n = 19$; Supporting Information Table 1).

Sera from patients with breast cancer were obtained from two sources. We obtained 193 sera from ISPY (TNBC $n = 50$; HER2+ $n = 68$; ER+ $n = 75$; subsets of this sera set were used for various assays) (ACRIN 6657, CALGB 150007/12) and 60 sera from Fox Chase Cancer Center (FCCC). Sera were derived from early-stage breast cancer patients from FCCC (HER2+ $n = 30$); control sera ($n = 30$) were gender matched (Supporting Information Table 1). All samples were obtained at the time of routine mammography, prior to diagnosis of cancer, and were selected retrospectively.

Written and informed consent was obtained from all subjects under institutional review board approval.

A gene expression signature predictive of p53 genotype was used to classify, breast tumors as p53 WT or mutated [16]. Deep sequencing of DNA samples from surgically resected pancreatic tumors, and correlation with *TP53* mutation status was performed at the UNMC tissue sciences facility. Tissues were formalin fixed and paraffin embedded, DNA was isolated using Qiagen DNeasy Tissue Kit, the *TP53* gene encompassing the exons was amplified by PCR, the products were purified and subjected to library generation according to the manufacturer's instructions (Illumina Inc.) for next-generation sequencing utilizing the Illumina Hi-Seq 2000 instrument in the UNMC Next Generation Sequencing Core Facility.

2.2 DNA preparation and cloning of mutant p53 and p53 fragments

Sequence-verified, full-length cDNA expression plasmids in the T7-based mammalian expression vector pANT7_cGST were obtained from Arizona State University's Biode-sign Institute Plasmid Repository and are publically available through DNASU (http://dnasu.asu.edu/DNASU/). The high-throughput preparation of high-quality supercoiled DNA for cell-free protein preparation was performed as described [15, 17]. Purified DNA is used in the generation of NAPPA p53 protein microarrays.

Cloning of the 51 p53 point mutant and p53 deletion and tiling fragments was performed from WT p53_pDONR221 (DNASU Plasmid ID: HsCD00001270). To create the 51 mutant p53 genes, overlapping oligonucleotides were designed with the most common single nucleotide change corresponding to the amino acid at that particular position (Fig. 2B). To create the p53 fragments, oligonucleotides were designed to remove sequentially 60 nucleotides from the 5′ prime (N-terminal deletions, NTD) end or the 3′ prime (C-terminal deletions, CTD) end of TP53, containing partial attA and attB cloning sites. The 12 tiled fragments (TF), each contained 144 nucleotides of p53, overlapping by 48 nucleotides, and spanning the p53 molecule were cloned (Supporting Information Table 2). The p53 mutagenesis fragments were cloned by PCR, and primer extension was performed using primary oligonucleotides. The final PCR product was subcloned into the pDONR221 vector and transformed in DH5α cells (Invitrogen, Carlsbad, USA). All clones were sequence verified prior to expression. A schematic of the p53 constructs is shown in Fig. 3.

2.3 Immunoblotting

WT p53 full-length and other modified constructs were expressed as described below using Hela lysate (Thermo Scientific, Rockford, IL). After expression 5 μL of the recombinant protein was run on a 10% SDS-PAGE gel and transferred to a PVDF membrane. The membrane was then probed with anti-GST MAb (Cell Signaling Technology, Danvers, MA), anti-p53 MAb DO.1, DO.14, and p240 (Santa Cruz Biotechnology, Santa Cruz, CA, USA) at 1:1000 dilutions and signal was developed using Supersignal West Pico Chemiluminiscent substrate (Pierce, Rockford, IL, USA).

2.4 Generation and screening of NAPPA p53 protein microarrays

The custom arrays were prepared by printing purified plasmid DNA essentially as described in [15]. Expression plasmid DNA (1500 ng/μL) was printed along with the capture antibody (anti-GST antibody, 50 ng/μL, Amersham, Fairfield, USA), protein cross-linker (BS^3, 2 mM, Pierce, Rockford, USA), and bovine serum albumin (3 mg/mL). Printing was done using a Genetix arrayer with 300 μm solid pins to have six equally printed subarrays per slide. p53 full length and 12 tiling fragments were printed in duplicate while all deletion fragments were printed as single spots. Water, printing buffer, and pANT7_GST empty vector were also printed as negative controls. Immobilized DNA was assessed with PicoGreen® staining (Invitrogen, Carlsbad, CA). Protein expression was assessed with detection of the anti-GST antibody (Cell Signaling Technologies, Danvers, MA). Quality was determined by correlating DNA and protein expression of two randomly chosen slides based on their R^2 value. Custom NAPPA slides were expressed and screened, without modifications, as previously described [18], and median fluorescence intensities (MFI) for each spot calculated.

The protein array data discussed in this manuscript have been deposited in the National Center for Biotechnology Information's Gene Expression Omnibus (GEO) and are accessible through GEO Series accession number GSE77949 (http://www.ncbi.nlm.nih.gov/geo/query/acc.cgi?acc=GSE77949).

2.5 RAPID ELISA

RAPID ELISA was performed as previously described in [19], with the following modifications. During incubation the patient serum was diluted (Pancreas 1:500, Ovarian 1:750, and Breast 1:100) in 100% *E. coli* lysate. Plates were developed using Supersignal ELISA Femto Chemiluminescent Substrate (Thermo Scientific). Relative luminescence units (RLU) were measured on a Glomax 96 Microplate Luminometer (Promega, Madison, WI) within 1–5 min of development.

2.6 Statistical analysis

For NAPPA, each array was first normalized by removing the background signal estimated by the first quartile of the nonspots and the log-transforming median-scaled raw intensities to bring the data to the same scale and stabilize the variance across the range of signals. For RAPID ELISA, all assays were performed in duplicate, and values plotted as mean values. Ratios were calculated using the MFI or RLU of a specific antigen over MFI or RLU control GST-protein, respectively. To determine significance we performed two-tailed *t* test.

3 Results

3.1 Frequency of WT-p53 AAb in SOC, PDAC, and BC serum

To determine the frequencies of p53-AAb in cancer patient's sera by RAPID ELISA, we expressed WT-p53 protein as a C-terminal GST fusion protein using mammalian cell lysate. We measured bound IgG in the sera from SOC (case $n = 17$, healthy control $n = 19$), PDAC (case $n = 45$, benign disease control $n = 43$), and three BC subtypes (TNBC case $n = 50$, HER2+ $n = 98$, and ER+ $n = 75$; healthy controls $n = 30$). Supporting Information Table 1

shows the age distribution, race, and gender of the cases and controls selected for these studies. A cutoff value was established as the mean of all the controls + 3SDs (cutoff, 2.045 at 94% specificity). Using this cutoff, p53-AAb were detected in 10/17 SOC cases (p = 0.0032, 58.8% sensitivity), 10/45 PDAC cases (p = 0.1121, 22.2% sensitivity), 16/50 TNBC cases (p = 0.0006, 32% sensitivity), 10/98 human epidermal growth factor receptor positive breast cancer (HER2+) BC cases (p = 0.0045, 10.2% sensitivity), and 3/75 ER+ BC cases (p = 0.5070, 4% sensitivity) (Fig. 1A). We observed the lowest frequency of p53-AAb in estrogen receptor positive breast cancer (ER+) breast cancer patients, consistent with a lower frequency of p53 mutations. We observed a difference in the strength of the signal depending on the tumor type. Both the intensity and frequency of p53-AAb was highest in tumors with higher predicted frequencies of *TP53* mutation (i.e. TNBC (50%) >HER2 (30%) >ER+ (22%)) [20] (Fig. 1A, breast) as well as observed in our sample set (Supporting Information Table 1).

3.2 Comparison of p53 autoantibodies in patients with WT versus mutant *TP53*

Based on these and previously published findings [10,21], we hypothesized that patients with sequence confirmed somatic mutations in *TP53* would have an increased frequency of p53-AAb. To determine if p53-AAb is associated with tumor *TP53* mutation, we used a different cohort of PC and BC patients with paired serum and tumor tissue samples. We obtained p53 mutation status from 44 PC and 137 BC tumor samples. Twenty-four PDAC and 89 BC tumors had sequence confirmed mutations in *TP53*, primarily consisting of single point mutations within the DNA-binding domain (Tables 1 and 2). IgG antibodies to WT-p53 were measured in 44 PC cases (20 WT-p53, 24 mutant p53) and 137 BC cases (48 WT-p53, 89 mutant p53). There was a trend toward an association of p53-AAb with tumor p53 mutation status for PDAC (PDAC WT mean 4.628 versus mutant mean 40.79, p = 0.0612; BC WT mean 1.487 versus mutant mean 2.614, p = 0.2874) (Fig. 1B). We observed 4/20 p53-AAb in serum from patients with WT-p53 tumor status, which may reflect other mechanisms of immunogenicity, or intratumoral heterogeneity of *TP53* mutations.

3.3 Generation of custom mutant p53 protein microarrays

Mutations in *TP53* can induce conformational changes of the WT-p53 protein [22]. Structural changes result in an extended half-life and accumulation of the mutant p53 protein, an important component of the humoral response [13]. To determine if p53-AAb are specific to mutant p53 protein epitopes, we constructed high-density NAPPA protein arrays displaying 51 p53 mutant proteins alongside 470 cancer-related proteins (Fig. 2A–C; Supporting Information Table 5). Printing of the DNA was uniform across the arrays, as measured by picogreen (Fig. 2A, left). The coefficient of variation for DNA content between replicate spots was less than 5%. Protein expression was confirmed by anti-GST antibody that detects the C-terminal GST fusion protein (Fig. 2A, right). Slide processing for protein display was uniform and reproducible between replicates within an array (R^2 = 0.95) and between duplicate arrays (R^2 = 0.96; data not shown).

3.4 Identification of mutant p53-specific antibodies

Using custom p53 mutation NAPPA arrays, we determined the frequency of mutant p53-AAb in PDAC patient sera (cases n = 60, benign disease controls n = 63). p53-AAb were

broadly reactive to the entire panel of expressed mutant p53 proteins (Fig. 2C, right images, Supporting Information Table 5) (Arg249Met, 20%; Arg213Leu, 17.6%; Pro278Ser, 20.6%; Gly187Ser, 17.2% sensitivities at 95% specificity). To determine if the p53-AAb were specific for mutant p53's we compared the four most immunogenic mutants using RAPID ELISA in sera from a randomly selected subset of the PDAC samples (case $n = 45$, benign disease control $n = 43$) and SOC (case $n = 17$, healthy control $n = 19$). A cutoff value was established as the mean of the controls + 2SD. Using this cutoff, the best performing p53 mutant (Arg249Met) provided the same sensitivity and specificity as WT-p53 in both PDAC and SOC (PC, 15.5% and OC, 58.8% sensitivity at PDAC, 95.3% and SOC, 89.4% specificity) (Fig. 2D; Supporting Information Fig. 1A).

3.5 Generation of a p53 epitope array for epitope mapping

To determine the epitope specificity, we designed deletion and tiling fragments of WT-p53 for fine epitope mapping. We generated 50 p53 constructs (19 NTD, 19 CTD, 12 TF, and full-length WT-p53, Fig. 3A). All clones were sequence verified prior to expression. Six of the p53 constructs (NTD20, NTD120, CTD20, CTD100, and CTD160), as well as full-length WT-p53 and control vector were probed by immunoblotting using anti-GST (Fig. 3B). The expected decrease in size with successive NTD and CTD deletions is shown. Epitopes of the p53 mAbs DO.1 and DO.14 are located between amino acids (AA) 21–25 and 56–65, respectively, which are deleted in NTD120. All fragments except NTD120 were detected by DO.1 and DO.14.

Then, to confirm epitope display, we mapped p53 using NTD and CTD deletion fragments and the p53 tiled fragments with the p53 mAb DO.1, DO.14, and p240 (AA 156–214) (Fig. 3C), using the anti-GST mAb as expression control (data not shown) and. As expected the p53 mAb DO.1 was able to identify all of the CTD (data not shown) as well as TL1 (AA 1–48) while none of the NTD (data not shown) as well as TL2-12 were able to be detected (Fig. 3C). Further, the p53 mAb DO.14 and p240 selectively recognized the TL 2 (AA 32–80) and TL7 (AA 192–240) (Fig. 3C).

3.6 Epitope mapping of p53 autoantibodies in patient sera

We used the p53 deletion arrays to map the linear immunogenic regions of p53. We screened 67 sera from patients that were strongly positive for WT p53-AAb by RAPID ELISA (PDAC $n = 13$, SOC $n = 14$, and BC (TNBC $n = 19$; Her2+ $n = 11$)) against TL1-12 fragments (48 AA each). Based on published literature [10], we hypothesized that the most immunogenic regions would be in the N- (1-94 AA, TL1-2) and C-terminus (323-393 AA, TL10-12) of p53 outside the central domain (100–300 AA, TL3-9). Regardless of the tumor type we identified TL1 and 2, in the N-terminus, as the most immunogenic regions (Fig. 4A–D; Supporting Information Table 3). OC and triple-negative breast cancer (TNBC) had similar broad immunogenic response to p53 including TL1, 2, 6, 7, 9, 10, and 12 (Fig. 4B–C).

To detect structural epitopes, we screened samples that exhibited a very strong WT p53-AAb response PDAC ($n = 2$), SOC ($n = 9$), and TNBC ($n = 3$) against both discontinuous (NTD and CTD) and continuous (TL) epitopes recognized by anti-p53 AAb (Fig. 5; Supporting

Information Table 4). Sera from all tumor types display a similar immunoprofile against the CTD and NTD constructs. Consistent with our TL data (Fig. 4), p53 CTD constructs have the highest signal on the array. This suggests there is an immunodominant epitope within the first 20 amino acids at the N-terminus of p53 leading to broad reactivity along the CTD constructs. As the first 20 amino acids were deleted from the first NTD deletion fragments from the N-terminus (NTD20) there is a complete loss in AAb signal, confirming this immunodominant epitope. There is a strong antibody signal from NTD61-180 within the DNA-binding domain, after which the signal diminishes. The NTD-300-380 signals demonstrate a subdominant epitope in the C-terminus (Fig. 5). These data demonstrate that there is a highly conserved antibody response to p53, despite the tumor type or mutation. The identification of AAb in the central domain of p53 is likely due to unmasked structural epitopes that are displayed on these arrays.

We sought to determine if any of the CTD fragments could outperform WT-p53 as an antigen for p53-AAb. We performed RAPID ELISA against the five most immunoreactive CTD constructs (CTD40, CTD200, CTD220, CTD280, and CTD300) for PDAC (case n = 45, benign disease control n = 43) and four CTD constructs (CTD80, CTD200, CTD240, and CTD260) for SOC (case n = 17, control n = 19) as well as WTp53 (Supporting Information Fig. 1B). A cutoff value was established as the mean of the controls + 2SD. Using this cutoff, the best performing CTD (PC, CTD40; OC, CTD80) provided the same sensitivity and specificity as WT-p53 in both PDAC and SOC (PDAC, 14.5% and SOC, 52.6% sensitivity at PDAC, 96.6% and SOC, 95% specificity). While there is a significant antibody response in both PDAC and SOC against all of the CTD as well as WT-p53 compared to controls. In summary, the linear epitopes do not improve detection of p53 AAb in these samples.

4 Discussion

In this study, we explored the utility of serum AAb against WT-p53 as a biomarker to distinguish malignant SOC, PDAC, and BC (TNBC, HER2+, and ER+) cancer from healthy and benign disease controls. A total of 488 patients from multiple tumor types were screened for the presence of serum AAbs against the p53 protein. Our study demonstrated that a significant subset of patients with SOC, PDAC, TNBC, HER2+ breast cancers have p53-AAbs, with sensitivities ranging from 10.2–58.8% at 94% specificity. We then created custom protein microarrays expressing overlapping TF, NTD, and CTD constructs against WT-p53 to map continuous and discontinuous immunogenic epitopes. In agreement with previous studies we identified immunogenic linear epitopes within the first 20 amino acids of the N-terminus and the last 60 amino acids of the C-terminus. We have also identified highly conserved immunogenic conformational epitopes within the DNA-binding domain. However, we do not observe any mutation-specific p53-AAbs.

4.1 p53 and its value as a biomarker

TP53 mutations are found in 50% of all human cancers and up to 30% of patients have circulating AAb [7], with a higher frequency in SOC (97%), PDAC (75%), and TNBC (74%) [20,23,24]. However, using traditional ELISA assays less than 20% of patients with

TP53 tumor mutations have circulating AAb to WT-p53 [10]. In these highly selected samples we observed sensitivities of 20–59%, respectively. In all cases the sensitivity of our assay was equal to or higher than previous reports (SOC, 16–30%; PDAC, 10.9%; TNBC, 19% [7]. Our SOC and PDAC samples were obtained from patients with late-stage disease that increases both Ab frequency and intensity [8]. To our knowledge, this is the first study to demonstrate the utility of p53 serum AAbs to discriminate malignant and benign pancreatic disease. Previous studies detected 10.9% of patients with p53 AAbs and were not able to distinguish malignant from benign disease [25–27]. We identified a trend between circulating AAbs to p53 and the presence of somatic tumor *TP53* mutations. Further validation with a larger cohort of samples and comprehensive sequencing of distant metastatic sites is warranted [28–30] (Fig. 1B).

4.2 Epitope mapping p53-specific antibodies

Epitope presentation is critical for serologic assays [31]. Since ovarian, pancreatic, and breast cancers have distinct patterns of p53 mutations we hypothesized that we would observe differences in the p53-derived immunogenic epitopes between these cancers. Prior studies, using overlapping linear constructs, have identified the N- and C-terminus as the immunodominant epitopes within p53 [10,11]. The N- and C- termini are hydrophilic segments located at the protein surface, which may explain its immunodominance. We constructed arrays containing both 12 continuous and 50 structural fragments of p53 to identify both linear and conformational-dependent epitopes. Our data confirm the strong immunodominant epitope at the N-terminus, and a weaker epitope at the C-terminus. We also detected a conformational-dependent epitope within the DNA-binding domain that is highly conserved within and between tumor types, regardless of the patient's mutation status. This is unmasked by deletion of the N-terminal 60 amino acids (NTD61) (Fig. 5). In SOC and TNBC, two genetically similar tumor types, we observed further conformational epitopes in the C-terminus at NTD300 and NTD360 (Fig. 5). Although the mutated DNA-binding domain region is buried within the molecule, differential folding of the 3D structure, could lead to the presentation of internal epitopes.

4.3 Diversity of immunogenicity for p53

To our knowledge, this is the most comprehensive epitope analysis of any cancer autoantigen. From the immunoprofile, there were two observations: (1) there is broad variability in detection of p53-AAb and (2) among the patients with AAb to p53, regardless of tumor type; they have a very similar immunoreactive profile. p53 AAbs are developed in patients with tumor p53 accumulation, but accumulation is not sufficient for the generation of an immune response, as over-expression of p53 in tumors induces humoral p53-specific immunity in only a minority of cancer patients. For example, the humoral immune response to vaccinia varies between individuals [32]. The heterogeneity could likely result from the diversity of HLA Class II alleles and CD4 T-helper cell epitopes stimulating B-cell Ab production [32].

The similarity in the polyclonal response to p53, regardless of tumor type or specific mutation, can be attributed to the intrinsic disorder or thermodynamic instability of p53. In healthy individuals p53 is rapidly degraded. In the absence of DNA the p53 tetramer is

thermodynamically unstable and extended allowing the N- and C-termini to interact with hundreds of proteins with high specificity but low affinity [33]. It has been shown that mutations in p53 lead to a more disordered protein with persistence of the extended state that may enhance for the presentation of immunogenic regions [13, 33].

Microarray technology has its advantage in high throughput, low sample requirement and capacity of simultaneously testing many target proteins at the same time. The method described here provides a new strategy for rapid epitope mapping of autoantibody responses. Methods such as this are necessary to understand the mechanisms of B-cell immunogenicity, and to improve algorithms that predict immunogenic B-cell epitopes.

Acknowledgments

This study was funded by the NCI R21 CA164593 (K.S.A. and M.A.H.) and the NCI Early Detection Research Network U01 CA117374 (K.S.A and J.L.). Rodrigo Barderas was supported by the Ramón y Cajal programme of the MINECO (Spain).

Dr. Anderson and Dr. LaBaer serve as a consultants and members of the scientific advisory board for ProvistaDx.

Abbreviations

AA	amino-acid
AAb	autoantibody
BC	breast cancer
CTD	C-terminal deletions
ER+	estrogen receptor positive breast cancer
HER2+	human epidermal growth factor receptor positive breast cancer
MFI	median fluorescence intensities
NAPPA	nucleic acid programmable protein arrays
NTD	N-terminal deletions
PDAC	pancreatic ductal adenocarcinoma
SOC	serous ovarian cancer
TF	tiling fragments
TNBC	triple-negative breast cancer
WT	wild-type

References

1. Murphy MA, O'Leary JJ, Cahill DJ. Assessment of the humoral immune response to cancer. J Proteomics. 2012; 75:4573–4579. [PubMed: 22300580]

2. Reuschenbach M, von Knebel Doeberitz M, Wentzensen N. A systematic review of humoral immune responses against tumor antigens. Cancer Immunol Immunother. 2009; 58:1535–1544. [PubMed: 19562338]

3. Yagami H, Kato H, Tsumoto K, Tomita M. Monoclonal antibodies based on hybridoma technology. Pharm Patent Analyst. 2013; 2:249–263.

4. Freed-Pastor WA, Prives C. Mutant p53: one name, many proteins. Genes Dev. 2012; 26:1268–1286. [PubMed: 22713868]

5. Anderson KS, Sibani S, Wallstrom G, Qiu J, et al. Protein microarray signature of autoantibody biomarkers for the early detection of breast cancer. J Proteome Res. 2011; 10:85–96. [PubMed: 20977275]

6. Anderson KS, Wong J, Vitonis A, Crum CP, et al. p53 autoantibodies as potential detection and prognostic biomarkers in serous ovarian cancer. Cancer Epidemiol Biomark Prev. 2010; 19:859–868.

7. Suppiah A, Greenman J. Clinical utility of anti-p53 auto-antibody: systematic review and focus on colorectal cancer. World J Gastroenterol. 2013; 19:4651–4670. [PubMed: 23922463]

8. Anderson KS, Cramer DW, Sibani S, Wallstrom G, et al. Autoantibody signature for the serologic detection of ovarian cancer. J Proteome Res. 2014; 14:578–586. [PubMed: 25365139]

9. Jaras K, Anderson K. Autoantibodies in cancer: prognostic biomarkers and immune activation. Expert Rev Proteomics. 2011; 8:577–589. [PubMed: 21999829]

10. Soussi T. p53 antibodies in the sera of patients with various types of cancer: a review. Cancer Res. 2000; 60:1777–1788. [PubMed: 10766157]

11. Lubin R, Schlichtholz B, Bengoufa D, Zalcman G, et al. Analysis of p53 antibodies in patients with various cancers define B-cell epitopes of human p53: distribution on primary structure and exposure on protein surface. Cancer Res. 1993; 53:5872–5876. [PubMed: 8261396]

12. Pedersen JW, Gentry-Maharaj A, Fourkala EO, Dawnay A, et al. Early detection of cancer in the general population: a blinded case-control study of p53 autoantibodies in colorectal cancer. Br J Cancer. 2013; 108:107–114. [PubMed: 23169294]

13. Joerger AC, Fersht AR. The tumor suppressor p53: from structures to drug discovery. Cold Spring Harbor Persp Biol. 2010; 2:a000919.

14. Anderson KS, Ramachandran N, Wong J, Raphael JV, et al. Application of protein microarrays for multiplexed detection of antibodies to tumor antigens in breast cancer. J Proteome Res. 2008; 7:1490–1499. [PubMed: 18311903]

15. Ramachandran N, Raphael JV, Hainsworth E, Demirkan G, et al. Next-generation high-density self-assembling functional protein arrays. Nat Methods. 2008; 5:535–538. [PubMed: 18469824]

16. Esserman LJ, Berry DA, Cheang MC, Yau C, et al. Chemotherapy response and recurrence-free survival in neoadjuvant breast cancer depends on biomarker profiles: results from the I-SPY 1 TRIAL (CALGB 150007/150012; ACRIN 6657). Breast Cancer Res Treat. 2012; 132:1049–1062. [PubMed: 22198468]

17. Qiu J, LaBaer J. Nucleic acid programmable protein array a just-in-time multiplexed protein expression and purification platform. Methods Enzymol. 2011; 500:151–163. [PubMed: 21943897]

18. Wang J, Barker K, Steel J, Park J, et al. A versatile protein microarray platform enabling antibody profiling against denatured proteins. Proteomics Clin Appl. 2013; 7:378–383. [PubMed: 23027520]

19. Wong J, Sibani S, Lokko NN, LaBaer J, Anderson KS. Rapid detection of antibodies in sera using multiplexed self-assembling bead arrays. J Immunol Methods. 2009; 350:171–182. [PubMed: 19732778]

20. Cancer Genome Atlas N. Comprehensive molecular portraits of human breast tumours. Nature. 2012; 490:61–70. [PubMed: 23000897]

21. Leroy B, Fournier JL, Ishioka C, Monti P, et al. The TP53 website: an integrative resource centre for the TP53 mutation database and TP53 mutant analysis. Nucleic Acids Res. 2013; 41:D962–D969. [PubMed: 23161690]

22. Muller PA, Vousden KH. p53 mutations in cancer. Nat Cell Biol. 2013; 15:2–8. [PubMed: 23263379]

23. Cancer Genome Atlas Research N. Integrated genomic analyses of ovarian carcinoma. Nature. 2011; 474:609–615. [PubMed: 21720365]
24. Weinstein JN, Collisson EA, Mills GB, et al. Cancer Genome Atlas Research N. The Cancer Genome Atlas Pan-Cancer analysis project. Nat Genet. 2013; 45:1113–1120. [PubMed: 24071849]
25. Laurent-Puig P, Lubin R, Semhoun-Ducloux S, Pelletier G, et al. Antibodies against p53 protein in serum of patients with benign or malignant pancreatic and biliary diseases. Gut. 1995; 36:455–458. [PubMed: 7698709]
26. Marxsen J, Schmiegel W, Roder C, Harder R, et al. Detection of the anti-p53 antibody response in malignant and benign pancreatic disease. Br J Cancer. 1994; 70:1031–1034. [PubMed: 7947080]
27. Raedle J, Oremek G, Welker M, Roth WK, et al. p53 autoantibodies in patients with pancreatitis and pancreatic carcinoma. Pancreas. 1996; 13:241–246. [PubMed: 8884844]
28. Segawa Y, Kageyama M, Suzuki S, Jinno K, et al. Measurement and evaluation of serum anti-p53 antibody levels in patients with lung cancer at its initial presentation: a prospective study. Br J Cancer. 1998; 78:667–672. [PubMed: 9744508]
29. Hammel P, Leroy-Viard K, Chaumette MT, Villaudy J, et al. Correlations between p53-protein accumulation, serum antibodies and gene mutation in colorectal cancer. Int J Cancer. 1999; 81:712–718. [PubMed: 10328221]
30. Blanchard P, Quero L, Pacault V, Schlageter MH, et al. Prognostic significance of anti-p53 and anti-KRas circulating antibodies in esophageal cancer patients treated with chemoradiotherapy. BMC Cancer. 2012; 12:119. [PubMed: 22448886]
31. Murphy MA, O'Connell DJ, O'Kane SL, O'Brien JK, et al. Epitope presentation is an important determinant of the utility of antigens identified from protein arrays in the development of autoantibody diagnostic assays. J Proteomics. 2012; 75:4668–4675. [PubMed: 22415278]
32. Duke-Cohan JS, Wollenick K, Witten EA, Seaman MS, et al. The heterogeneity of human antibody responses to vaccinia virus revealed through use of focused protein arrays. Vaccine. 2009; 27:1154–1165. [PubMed: 19146908]
33. Maslon MM, Hupp TR. Drug discovery and mutant p53. Trends Cell Biol. 2010; 20:542–555. [PubMed: 20656489]

Clinical Relevance

We have used in vitro programmable protein array technology as a novel strategy to map both continuous and discontinuous B-cell immunogenic epitopes. Currently, bioinformatics tools to predict B-cell epitopes have been unsuccessful and have not properly considered the sequence composition as well as the 3D structure of the protein. The ability to map both continuous and discontinuous B-cell immunogenic epitopes from serum antibodies has significant clinical relevance in understanding B-cell immunogenicity, developing more reliable epitope prediction algorithms, leading to the development of more efficient drug targets and the identification of biomarkers. Further utility of this strategy is needed to develop more reliable predictive models of immunogenic epitopes.

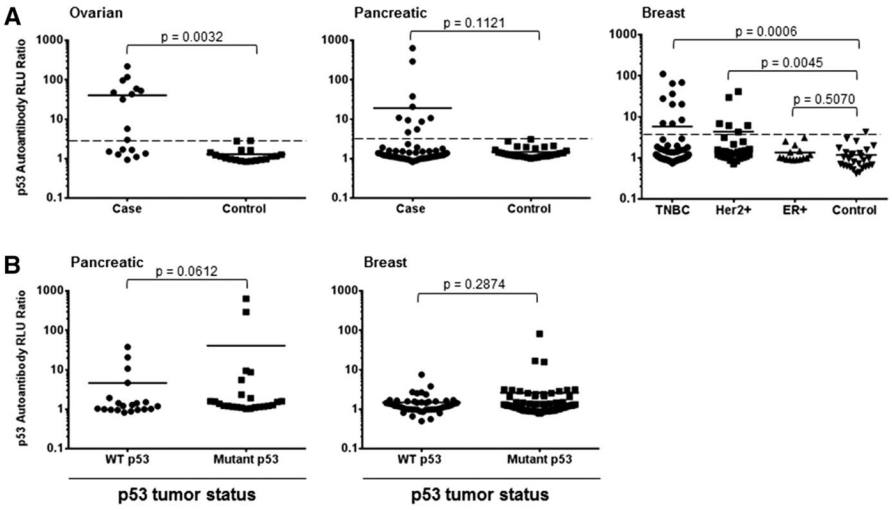

Figure 1.

p53 autoantibodies are highly specific biomarkers in multiple cancer types. (A) Column dot plots of sera from serous ovarian cancer patients ($n = 17$) and healthy controls ($n = 19$), pancreatic cancer patients ($n = 45$) and benign pancreatic disease controls ($n = 43$), triple negative breast cancer ($n = 50$), HER2+ breast cancer ($n = 68$), ER+ breast cancer ($n = 75$), and healthy controls ($n = 30$) were tested for p53-specific antibodies by RAPID-ELISA. The dotted line indicates the cutoff value (mean signal of controls + 3SD). (B) Column dot plots of sera from pancreatic cancer patients carrying WT-p53 ($n = 20$) or mutant p53 ($n = 24$) in the tumor tissue and from breast cancer patients carrying WT-p53 ($n = 47$) and mutant p53 ($n = 44$) tested for p53-specific antibodies by RAPID-ELISA. All results are presented as the ratio of RLU over GST background, where the solid line represents the mean on the column dot plots. *p*-values were calculated using a two-tailed *t*-test.

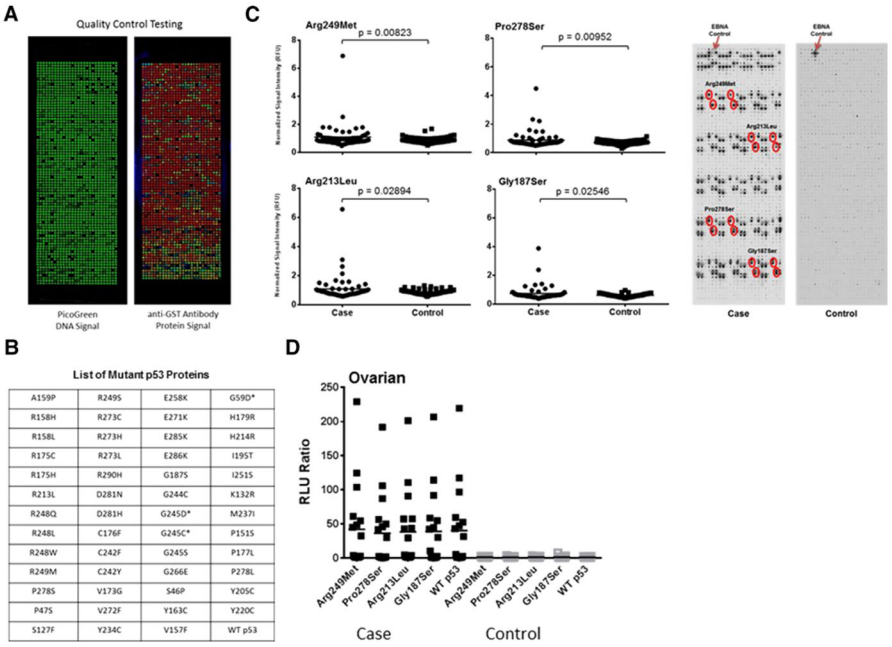

A159P	R249S	E258K	G59D*
R158H	R273C	E271K	H179R
R158L	R273H	E285K	H214R
R175C	R273L	E286K	I195T
R175H	R290H	G187S	I251S
R213L	D281N	G244C	K132R
R248Q	D281H	G245D*	M237I
R248L	C176F	G245C*	P151S
R248W	C242F	G245S	P177L
R249M	C242Y	G266E	P278L
P278S	V173G	S46P	Y205C
P47S	V272F	Y163C	Y220C
S127F	Y234C	V157F	WT p53

Figure 2.

p53-AAbs are broadly cross-reactive to mutant p53 proteins. (A) High-density nucleic acid programmable protein microarrays (NAPPA) displaying 51 recombinant mutant p53 as well as WT-p53 protein were probed with serum from pancreatic cancer ($n = 60$) and patients with benign pancreatic disease ($n = 63$). dsDNA was visualized by Picogreen and protein expression was detected using an anti-GST tag antibody. (B) List of p53 mutant proteins displayed on the array. The asterisk indicates point mutant p53 proteins that did not express. (C) Normalized sera antibody expression from pancreatic cancer (Cases; $n = 60$) and benign pancreatic disease (Control; $n = 63$) is presented for the four most immunogenic p53 mutants. *p*-values were calculated using two-tailed *t*-test. (D) Rapid-ELISA was performed to validate serum antibodies against four mutant p53 and WT-p53 in sera from serous ovarian cancer (case $n = 17$, control $n = 19$). The data is presented as relative light unit (RLU) ratio over background GST signal.

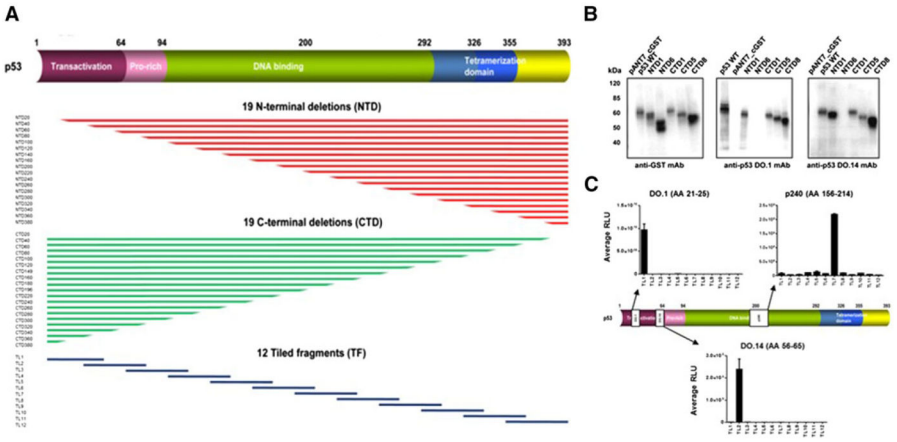

Figure 3.

Generation of a p53-epitope mapping protein array. (A) Truncated p53 constructs were designed with sequential and accumulative 20 amino acid deletions, alternatively from the N-terminal (NTD) or C-terminal (CTD). Tiled fragments of p53 were 48 amino acids in length. The fragments contain 16 amino acids overlapping the previous and the next tiled fragment spanning the wild type p53 protein. (B) Plasmid DNA coding for six randomly selected constructs and WTp53 were expressed in vitro and detected by immunoblot analysis with anti-GST mAb, and the anti-p53 mAb DO.1 and DO.14. (C) Plasmid DNA coding for TL1-12 were expressed and the specificity was verified using the anti-p53 mAb DO.1, DO.14, and p240 antibody.

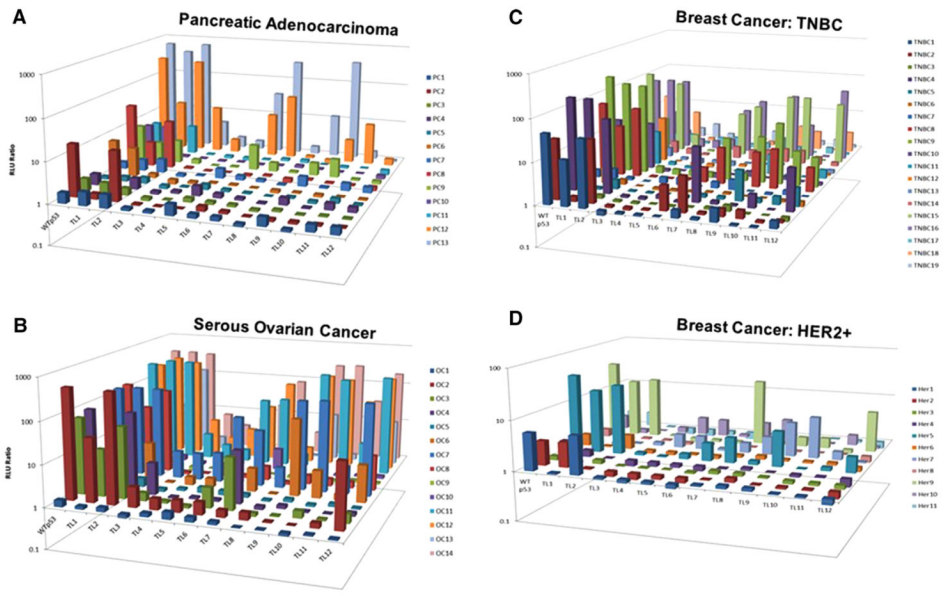

Figure 4.

Epitope mapping of patient sera using the p53 tiling array. Sera from (A) pancreatic adenocarcinoma (PC; $n = 13$), (B) serous ovarian cancer (OC; $n = 14$), (C) triple negative breast cancer (TNBC; $n = 19$), and (D) HER2+ breast cancer (Her2; $n = 11$) were tested by RAPID ELISA against 12 overlapping tiling fragments (TL1-12) spanning the entire length of WT-p53. Data are presented as relative light unit (RLU) ratio over background GST signal.

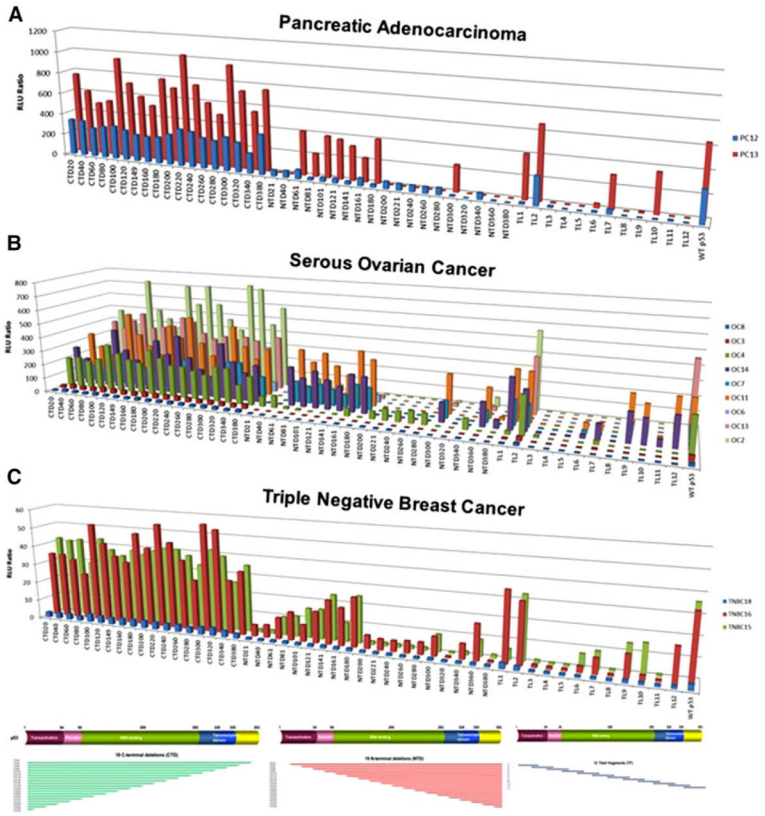

Figure 5.

Detection of linear and conformational p53 epitopes by patient sera display a unique and conserved pattern of antibody expression. A p53 epitope array expressing 19 N-terminal deletions, 19 C-terminal deletions, and 12 overlapping tiling fragments of WT-p53 was screened with sera and IgG was detected. (A) Pancreatic adenocarcinoma ($n = 2$), B) serous ovarian cancer ($n = 9$), and C) triple negative breast cancer ($n = 3$) sera were screened against 19 CTD, 19 NTD, 12 TL, and full-length WT-p53. The data is presented as relative light unit (RLU) ratio over background GST signal.

Table 1

Pancreatic adenocarcinoma patients sequenced for *TP53* mutations and normalized serum p53 autoantibody expression values determined by RAPID-ELISA

Pancreatic adenocarcinoma									
WT p53		**Mutant p53**						**Unknown p53 status**	
Case ID	**p53 AAb**	**Case ID**	**p53 AAb**	**N-term p53 mutation**	**Case ID**	**p53 AAb**	**Central p53 mutation**	**Case ID**	**p53 AAb**
7	1.9313	4	1.1705	N-Term; P146S	5	1.1563	Central; R117W	14	2.3346
9 (PC8)	37.8228	11	1.5612	N-Term; E39X	6	1.1267	Central; R150W	15 (PC6)	8.7276
10 (PC9)	10.7278	12	1.5216	N-Term; S51Stop	26	1.2121	Central; R116Q	56 (PC11)	5.4687
13	0.9972	16	1.1442	N-Term; R43H	27 (PC1)	1.0189	Central; R150W		
17	1.2886	19 (PC12)	293.6286	N-Term; R43H; G128A	33	1.0933	Central; G113S		
18	0.964	28	1.2703	N-Term; C44S	35	1.3819	Central; G134V		
20	4.6795	30 (PC10)	9.4811	N-Term; S34X	37	1.2246	Central; P146R		
21	0.9523	41	1.9045	N-Term; R43H	38	1.5943	Central; S109A		
23	0.9964	54 (PC13)	635.9295	N-Term; Q4E	39	5.5181	Central; N115I		
24 (PC5)	0.8782				46	1.0396	Central; Y126N		
25 (PC2)	20.7034				50	1.1111	Central; E126D		
29	0.97				22	1.2008	5′ UTR		
31	0.8253				44 (PC4)	1.5924	splicing: exon6; exon10		
32	1.5106				N-Term (N-Terminus, 1–94 AA) Central (Central Domain, 100–300 AA) C-Term (C-Terminus, 323–393 AA)				
34	1.0214								
40	1.1895								
43	1.4301								
45	1.0348								
48	1.4181								
49	1.2129								
52 (PC7)	1.4769								

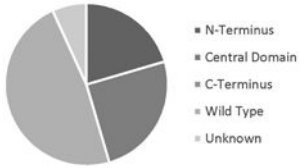

Table 2

Breast cancer patients sequenced for *TP53* mutations and normalized serum p53 autoantibody expression values determined by RAPID-ELISA

Breast adenocarcinoma				
WT p53		**Mutant p53**		
Case ID	**p53 AAb**	**Case ID**	**p53 AAb**	**p53 mutation status**
210236	0.4981	211160	1.0957	Central; S127T
211631	1.165	212115	0.93	Central; P151H
212063	0.9603	212314	0.7894	Central; R273C
213784	1.5765	214477 (TNBC19)	3.0472	Central; R175H
214443	1.2607	215632	0.9257	Central; R175H
215311	1.1168	215662	0.8726	Central; R273C
218398	1.6562	216716	0.9117	Central; R175H
218566	0.9992	216828 (TNBC16)	16.8121	Central; D259V
220460	0.9861	217569	1.1943	Central; P278A
221153	0.8586	218723 (TNBC17)	2.4085	Central; L130V
221197	1.1491	218813 (TNBC15)	82.182	Central; G245C
221855	0.6584	219487	0.8884	Central; R273H
221935	1.2002	221243	0.8956	Central; C242Y
222349	2.6672	224280	0.8549	Central; R175H
222600	1.6942	225637	1.2341	Central; R249S
222922	1.2183	225709	1.0835	Central; G245S
223062	7.5551	226664	1.3741	Central; E221stop
225739	0.8838	228173	2.5489	nt13054
225983	0.9922	228259 (Her11)	2.8728	Central; V173L
227330	1.465	228328 (TNBC14)	2.1465	Central; R272L
227424	1.4472	229435	1.1195	Central; Q165Stop
227447	1.3768	231390	0.9362	Central; Y236C
228351	1.0385	231663	0.9855	Central; R248G
231232	1.4972	231964	1.0004	Central; 1 bp ins codon 298
231482	0.9617	231971	1.3193	silent

Breast adenocarcinoma					
WT p53		Mutant p53			
Case ID	p53 AAb	Case ID	p53 AAb	p53 mutation status	
231537	0.8172	232149	1.4913	Central; R273P	
231757	1.0111	232840 (Her10)	2.0514	Central; R273H	
232588	1.3425	235186	1.3264	Central; Y107Stop	
235741	0.9767	237517 (TNBC18)	15.8366	Central; C135Y	
236843	1.5771	237775	0.9136	Central; Q136stop	
237457	1.3887	238179	0.9024	Central; R248W	
237713	2.3609	238589	1.0297	Central; R175H	
237953	1.56	238717	1.3495	Central; R273H	
238849	0.5576	239736	1.209	Central; R261S	
239012	3.8162	240416	1.0971	Central; M246V	
239107	1.1983	241385	1.2151	Central; Del. 1bp codon 151	
239359	2.5346	241400	1.1572	Central; C275F	
240238	1.0763	251142	3.1325	Central; Ins. 8bp codon 285	
241376	1.0012	252324	1.2849	Central; Q192Stop	
241397	0.7957	252470	1.2366	Central; G266E	
242787	2.7241	252476	1.4614	Central; P278L	
243160	0.9907	1021651	1.2988	Central; G145S	
243506	1.4377	1021957	0.8778	Central; R280T	
244361	0.9856	1021960	0.8984	Central; R175H	
251308	1.4414	1021975	1.0012	Central; E258G	
252446	1.5466				
252460	1.7104				
252466	1.6382				